



**HAL**  
open science

## Probing magnetic singularities during magnetization process in FePd films

Aurélien Masseboeuf, Thomas Jourdan, Frédéric Lançon, Alain Marty,  
Pascale Bayle-Guillemaud

► **To cite this version:**

Aurélien Masseboeuf, Thomas Jourdan, Frédéric Lançon, Alain Marty, Pascale Bayle-Guillemaud. Probing magnetic singularities during magnetization process in FePd films. Applied Physics Letters, 2009, 95 (21), pp.212501. 10.1063/1.3266825 . hal-00419559

**HAL Id: hal-00419559**

**<https://hal.science/hal-00419559v1>**

Submitted on 24 Sep 2009

**HAL** is a multi-disciplinary open access archive for the deposit and dissemination of scientific research documents, whether they are published or not. The documents may come from teaching and research institutions in France or abroad, or from public or private research centers.

L'archive ouverte pluridisciplinaire **HAL**, est destinée au dépôt et à la diffusion de documents scientifiques de niveau recherche, publiés ou non, émanant des établissements d'enseignement et de recherche français ou étrangers, des laboratoires publics ou privés.

# Probing punctual magnetic singularities during magnetization process in FePd films

Aurélien Masseboeuf,<sup>\*</sup> Thomas Jourdan,<sup>†</sup> Frédéric Lançon, Pascale Bayle-Guillemaud, and Alain Marty  
*CEA, INAC, SP2M, F-38054 Grenoble-, France*

(Dated: September 24, 2009)

## Abstract

We report the use of Lorentz microscopy to observe the domain wall structure during the magnetization process in FePd thin foils. We have focused on the magnetic structure of domain walls of bubble-shaped magnetic domains near saturation. Regions are found along the domain walls where the magnetization abruptly reverses. Multiscale magnetic simulations shown that these regions are vertical Bloch lines (VBL) and the different bubble shapes observed are then related to the inner structure of the VBLs. We were thus able to probe the presence of magnetic singularities as small as Bloch points in the inner magnetization of the domain walls.

It has been shown that alloys with perpendicular magnetic anisotropy (PMA) are good candidates for applications in new recording media with high density storage capacity or in magneto-logical devices<sup>1</sup>. Recently such materials, namely iron palladium (FePd) alloys have been used in spin-valves where they act as the polarizer and the free layer<sup>2</sup>. These devices are believed to work through the nucleation of a reversed domain followed by the propagation of a domain wall<sup>3</sup>. Numerous studies have advanced the knowledge of the magnetic configuration of FePd alloys by means of MFM imaging<sup>4,5</sup>, X-ray scattering<sup>6</sup>, or numerical simulations<sup>7</sup>. Moreover it has been shown recently that it is possible, using Lorentz Transmission Electron Microscopy (LTEM) to image the magnetic distribution in PMA thin foils at the domain wall scale<sup>8</sup>. This method enables quantitative information to be obtained with a spatial resolution below ten nanometers coupled to the opportunity of applying magnetic field during imaging. Here we show that it is also possible to probe the micromagnetic configuration inside the domain wall enabling the detection of defects smaller than the expected spatial resolution.

Along a domain wall one can find some regions where the chirality abruptly switches. The area where the magnetization reverses is called a Bloch line, which can be either horizontal or vertical. An horizontal Bloch line is parallel to the magnetization inside the domain wall while the vertical Bloch line is perpendicular to the magnetization. Domain walls in PMA materials are Bloch-like walls and the in-plane magnetization inside the domain wall can thus be oriented in one or the other direction of the wall plane and defines its chirality. We can thus expect some vertical Bloch lines in FePd delimiting two different chirality of the domain wall. Vertical Bloch lines were extensively studied in the 80s in garnets. Experimental<sup>9,10,11</sup> and numerical<sup>12,13,14,15</sup> approaches have helped us to understand these types of magnetic defects. Observations were possible using magneto-optical microscopy due to the large width of domain walls in garnets ( $\delta \approx 0.1 \mu\text{m}$ ). This large value has to be compared with the domain wall width in FePd of around 8 nm<sup>16</sup>, well below the resolution of optical methods. The simulation of the magnetic structure in garnets is also much easier than for FePd. Indeed, in garnets the very high quality factor  $Q = 2K/(\mu_0 M_s^2) \approx 8$ , where  $K$  is the anisotropy constant and  $M_s$  the saturation magnetization, enables local approximations for the computation of the demagnetizing field<sup>13</sup>. This assumption is *a priori* not valid in the case of FePd, which exhibits smaller values of  $Q$  in the order of 1.6.

The aim of this letter is to show that new magnetic modeling coupled to recent develop-

ments in LTEM enables the observation of such small magnetic defects as VBL in domain walls of less than 10 nm width. We focus in this work on VBL which are trapped in magnetic bubbles appearing in FePd thin foils near the saturation state.

A thin layer of L1<sub>0</sub>-FePd (37 nm) has been deposited on a “soft” layer of chemically disordered FePd<sub>2</sub> layer, grown on a MgO (001) substrate by Molecular Beam Epitaxy<sup>17</sup>. The soft layer is used to enhance the recording efficiency in perpendicular recording hard drives (see for example the section 2.4 of 18). The sample for LTEM has been then prepared using classical method by mechanical polishing and ion milling. The microscope used is a JEOL 3010 fitted in with a Gatan imaging filter for contrast enhancement by zero-loss filtering<sup>19</sup>. The *in-situ* magnetization is performed with the objective lens while imaging is realized with the objective mini lens traditionally used for low magnification imaging. The field produced by the objective lens has been carefully calibrated by inserting a dedicated sample holder mounted with a Hall probe before the experiment.

We measured the half hysteresis loop of the film in Fresnel mode<sup>20</sup>. For a field of 775 mT, just before the complete saturation of the magnetic layer, a focal series has been performed. The complete description of this magnetization process can be found elsewhere<sup>8</sup>. Fig. 1 shows the focal series reconstruction using the Transport-of-Intensity Equation<sup>21</sup>. The magnetic information is originally mixed with an electrostatic contribution<sup>22</sup> which has been removed by considering a constant variation of the thickness of the sample<sup>16</sup>. Due to the Lorentz force, the LTEM is sensitive to magnetic induction integrated along the electron beam direction in the TEM. However, assuming that stray fields on both side of the layer are antiparallel, the integrated induction may be considered approximately the same as the integrated magnetization. In the following we will discuss about simulation on integrated magnetization.

In Fig. 1 we can clearly see two types of magnetic bubbles. On the upper left corner one can see a magnetic bubble where the magnetization swirls continuously along the domain wall between the residual magnetic domain (indicated as down in Fig. 1) and the reversed domain. On the bottom right corner, one finds a magnetic bubble where the magnetization experiences two rotations of 180° resulting in two “different” domain walls pointing in similar directions.

At this point of the hysteresis loop a lot of bubbles are present in the film and both kinds of bubbles can be easily found. The two switching points observed in the second bubble

type are supposed to be vertical Bloch lines (VBL)<sup>23</sup>. It must be noticed that the geometric deformation observed for the bubble with two VBL (the bubble showing a *lemon* shape) is fully reproducible.

In order to investigate the internal structure of these lines, we have performed magnetic simulations on bubbles with and without VBL. Due to the large range of scale needed to model these objects, we developed and used a multiscale efficient method. This method uses an adaptive mesh refinement technique to achieve both computational efficiency and numerical accuracy (details on the method can be found in Ref. 24). This is particularly useful in the case of bubbles as the inner and outer part of the bubble can be loosely meshed, whereas the domain wall and the VBL must be densely meshed<sup>25</sup>. Moreover, the code we used has the particularity to take into account the atomic structure of the material which is ignored in standard micromagnetic codes. The size of the micromagnetic mesh is then automatically adapted and switch to atomistic mode to keep a good precision when necessary. This ensures that all magnetic configuration is correct as the micromagnetic fundamental assumption of low spatial variations is fulfilled (see 26 for more details and comparisons with traditional code) and at the same time decrease drastically the number of mesh (thus decreasing the calculation time). The following calculation would have cost 8 times more mesh with a traditional micromagnetic parallel code.

In these simulations the saturation magnetization is  $M_s = 10^6$  A.m<sup>-1</sup>, the anisotropy constant is  $K = 10^6$  J.m<sup>-3</sup> and the exchange stiffness constant<sup>27</sup> is  $A = 7 \times 10^{-12}$  J.m<sup>-1</sup>. With these parameters the exchange length,  $\Lambda = \sqrt{2A/(\mu_0 M_s^2)}$  = 3.3 nm. Two different thicknesses have been considered : 15 and 20.7 nm. In Fig. 2 the integrated magnetization along the thickness obtained from the simulations is shown for a bubble without VBL (A) and two bubbles with VBL for thicknesses of 15 (B) and 20.7 nm (C) in a field of 0.25 and 0.3 T respectively.

It can be seen that for a thickness of 15 nm (Fig. 2 B) the bubble is deformed in agreement with the LTEM observations, whereas for a thickness of 20.7 nm its shape remains circular (Fig. 2 C).

The modification of the shape can be explained by analysing precisely the structure of the VBL, depending of the thickness. Two kinds of VBL can thus be found. In the case of a small thickness, the magnetization is uniform along the VBL (Fig. 3 A), whereas it reverses along the VBL in the second case (large thickness), which leads to a magnetic singularity called

a Bloch point (BP) (Fig. 3 B). The reason for the transition is a competition between the exchange and demagnetizing energies: the presence of a Bloch point leads to an increase in the exchange energy, whereas the demagnetizing energy decreases because the magnetization in the two segments of the line is aligned along the stray field generated by the domains.

Such a transition as a function of the thickness,  $h$  has been reported by Hubert to be  $h = 7.3 \text{ \AA}$  with an analytical model for a straight domain wall<sup>28</sup>. According to our simulations for the particular geometry considered here, the transition is found between 4.5 and 6.3  $\text{\AA}$ . Given the thickness,  $h = 11.2 \text{ \AA}$  of the films observed by LTEM, the VBL should contain a Bloch point, which is not consistent with the deformed states observed. However, the soft layer under the  $L1_0$  FePd film changes the magnetic configuration and alters the respective contributions of the exchange and demagnetizing terms to the energy. As described in a previous article<sup>29</sup>, the main role of the soft layer on the domain wall is an enhancement of the size (and as a consequence, the thickness) of the bottom Néel cap of the Bloch walls. This vertical dissymmetry could thus favour the configuration with no BP by increasing the dipolar energy.

The deformation observed in the absence of a BP gives rise to a reduction of magnetic charges<sup>25</sup>: it is analogous to the small buckling of the magnetization identified in straight domain walls in garnets<sup>15</sup>. In these materials, the buckling reduces the so-called “dipolar”  $\pi$  charges which are related to the variation of the magnetization perpendicular to the domain wall. In the case of FePd, the lower quality factor,  $Q$  reduces the lateral extension of the VBL, which leads to large “monopolar”  $\sigma$  charges. A far larger buckling than could be expected following the studies on garnets is obtained, beside a reduction of  $\pi$  charges, it also reduces  $\sigma$  charges by a compensation of these two types of charges. It is worthy to note that the magnetization is oriented in the same direction in both VBL, so that the 360°-like domain walls are located on opposite surfaces. To compensate these charges, a different orientation in the VBL would lead to a “heart”-shape bubble, which is not found to be stable in our simulations.

To conclude, in this letter we have highlighted the very high resolution obtained by combining Lorentz Transmission Electron Microscopy and multiscale simulations. The resolution we achieved by conventional electron microscopy enables us to probe magnetic singularities well below the LTEM spatial resolution. Furthermore a main advantage of the multiscale code was its rapidity and its low memory requirements. In that particular case we decrease

the number cells thanks to a factor 8 regarding traditional parallel code. The successful comparison of the two methods shown that it is possible to determine the inner magnetic configuration of a VBL, namely the presence or the absence of Bloch points in them.

---

\* New ad. : CNRS, CEMES, F-31055 Toulouse Cedex, France

† New ad. : CEA, DEN, Service de Recherches de Métallurgie Physique, F-91191 Gif-sur-Yvette, France

- <sup>1</sup> D. Weller, A. Moser, L. Folks, M. E. Best, W. Lee, M. Toney, M. Schwickert, J.-U. Thiele, and M. Doerner, *IEEE Transaction on Magnetics* **36**, 10 (2000).
- <sup>2</sup> T. Seki, S. Mitani, K. Yakushiji, and K. Takanashi, *Applied Physics Letters* **88**, 172504 (pages 3) (2006).
- <sup>3</sup> T. Seki, S. Mitani, and K. Takanashi, *Physical Review B (Condensed Matter and Materials Physics)* **77**, 214414 (pages 8) (2008).
- <sup>4</sup> A. Asenjo, J. Garcia, D. Garcia, A. Hernando, M. Vazquez, P. Caro, D. Ravelosona, A. Ce-bollada, and F. Briones, *Journal of Magnetism and Magnetic Materials* **196**, 23 (1999), ISSN 0304-8853, 7th European Magnetic Materials and Applications Conference (EMMA 98), ZARAGOZA, SPAIN, SEP 09-12, 1998.
- <sup>5</sup> Y. Samson, A. Marty, R. Hoffmann, V. Gehanno, and B. Gilles, in *J. Appl. Phys.* (AIP, 1999), vol. 85, pp. 4604–4606.
- <sup>6</sup> M. Mulazzi, K. Chesnel, A. Marty, G. Asti, M. Ghidini, M. Solzi, M. Belakhovsky, N. Jaouen, J. M. Tonnerre, and F. Sirotti, *Journal of Magnetism and Magnetic Materials* **272-276**, E895 (2004), proceedings of the International Conference on Magnetism (ICM 2003).
- <sup>7</sup> J. C. Toussaint, A. Marty, N. Vukadinovic, J. B. Youssef, and M. Labrune, *Computational Materials Science* **24**, 175 (2002).
- <sup>8</sup> A. Masseboeuf, C. Gatel, A. Marty, J. C. Toussaint, and P. Bayle-Guillemaud, in *Journal of physics: conference series* (Institute of Physics Publishing, 2008), vol. 126, p. 012055.
- <sup>9</sup> A. Thiaville and J. Miltat, *Journal of Applied Physics* **68**, 2883 (1990).
- <sup>10</sup> A. Thiaville, J. B. Youssef, Y. Nakatani, and J. Miltat, 35th annual conference on magnetism and magnetic materials **69**, 6090 (1991).
- <sup>11</sup> A. Thiaville, J. Miltat, and J. Ben Youssef, *European Physical Journal B* **23**, 37 (2001).

- <sup>12</sup> A. Hubert, AIP Conference Proceedings **18**, 178 (1974).
- <sup>13</sup> J. C. Slonczewski, AIP Conference Proceedings **24**, 613 (1975).
- <sup>14</sup> Y. Nakatani and N. Hayashi, Magnetics, IEEE Transactions on **24**, 3039 (1988).
- <sup>15</sup> J. Miltat, A. Thiaville, and P. Trouilloud, Journal of Magnetism and Magnetic Materials **82**, 297 (1989).
- <sup>16</sup> A. Masseboeuf, C. Gatel, J. C. Toussaint, A. Marty, and P. Bayle-Guillemaud, Ultramicroscopy **In press**, doi:10.1016/j.ultramic.2009.08.006 (2009).
- <sup>17</sup> G. Beutier, A. Marty, K. Chesnel, M. Belakhovsky, J. Toussaint, B. Gilles, G. Van der Laan, S. Collins, and E. Dudzik, Physica B **345**, 143 (2004).
- <sup>18</sup> S. Khizroev and D. Litvinov, *Perpendicular Magnetic Recording* (Kluwer Academic Publishers, 2004).
- <sup>19</sup> J. Dooley and M. De Graef, Micron **28**, 371 (1997).
- <sup>20</sup> J. Chapman, Journal of Physics D : Applied Physics **17**, 623 (1984).
- <sup>21</sup> D. Paganin and K. Nugent, Physical review letters **80**, 2586 (1998).
- <sup>22</sup> Y. Aharonov and D. Bohm, Physical Review **115**, 485 (1959).
- <sup>23</sup> A. Hubert and R. Schäfer, *Magnetic Domains* (Springer, 1998).
- <sup>24</sup> T. Jourdan, A. Marty, and F. Lançon, Physical Review B **77**, 224428 (2008).
- <sup>25</sup> T. Jourdan, A. Masseboeuf, F. Lançon, P. Bayle-Guillemaud, and A. Marty, submitted to Journal of Applied Physics (2009).
- <sup>26</sup> T. Jourdan, Ph.D. thesis, Universit Joseph Fourier (2008).
- <sup>27</sup> V. Gehanno, A. Marty, B. Gilles, and Y. Samson, Physical Review B **55**, 12552 (1997).
- <sup>28</sup> A. Hubert, Journal of Magnetism and Magnetic Materials **2**, 25 (1976).
- <sup>29</sup> A. Masseboeuf, F. Cheynis, J. C. Toussaint, O. Fruchart, C. Gatel, A. Marty, and P. Bayle-Guillemaud, in *Materials Research Society Symposium Proceedings* (2007), vol. 1026, pp. 1026–C22.



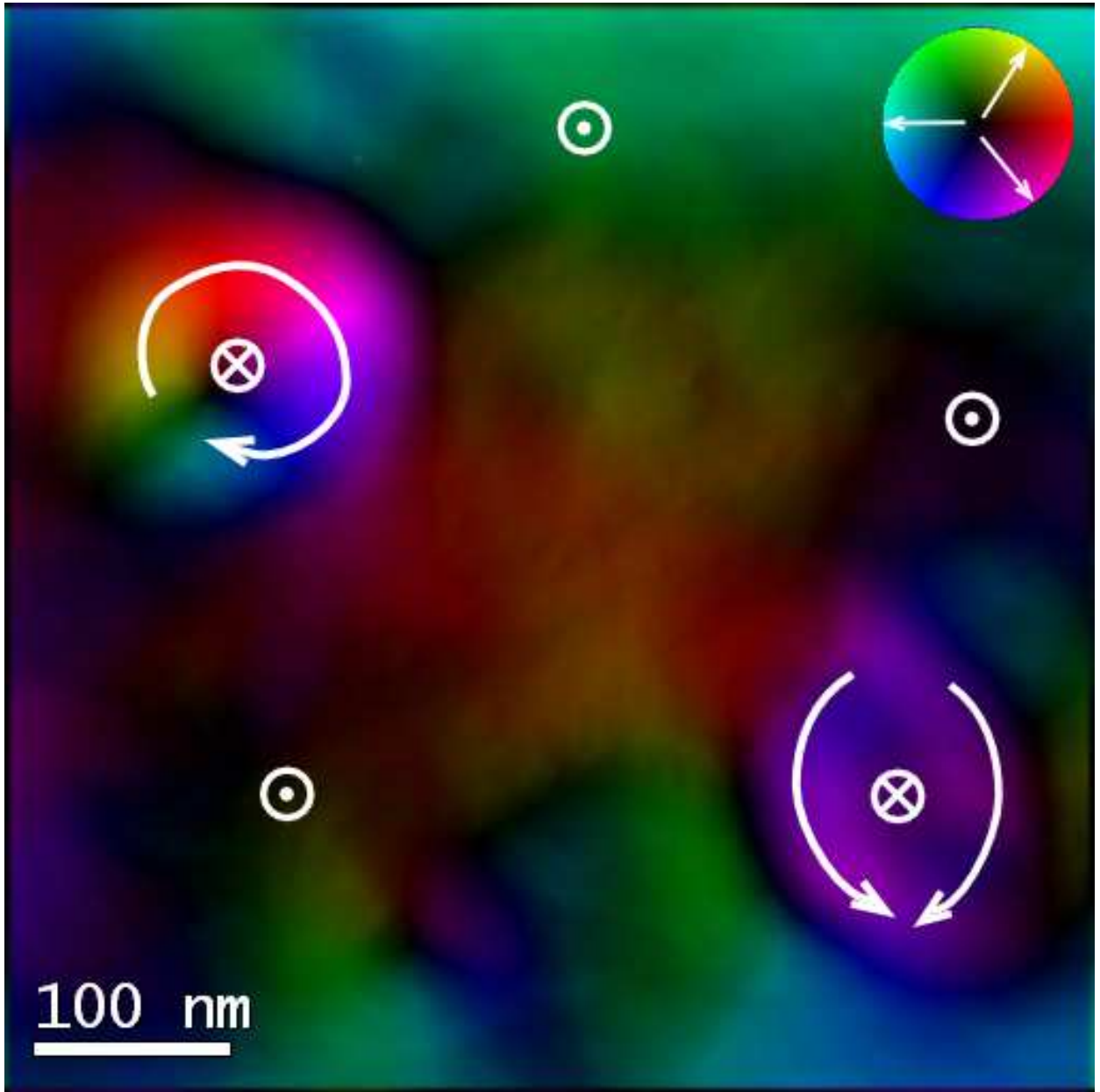


FIG. 1: (Colour online) Magnetic induction mapping of the FePd thin film using TIE solving at 775 mT. The colour scale used here is explained by the colour wheel (colour for the magnetic induction direction and colour intensity for the induction modulus). Arrows are also used to emphasize the magnetic induction. Perpendicular induction (*i.e.* magnetization inside the domains) is deduced from the whole magnetization process (saturation state should be up).

FIG. 2: Magnetic multi-scale simulations of three different magnetic bubbles. The magnetization has been integrated along the observation direction to correspond to LTEM measurements. (A) A magnetic bubble with no VBL. (B) A magnetic bubble with two VBL, both VBL contain no Bloch point. (C) A magnetic bubble with two VBLs, each VBL contains a Bloch point.

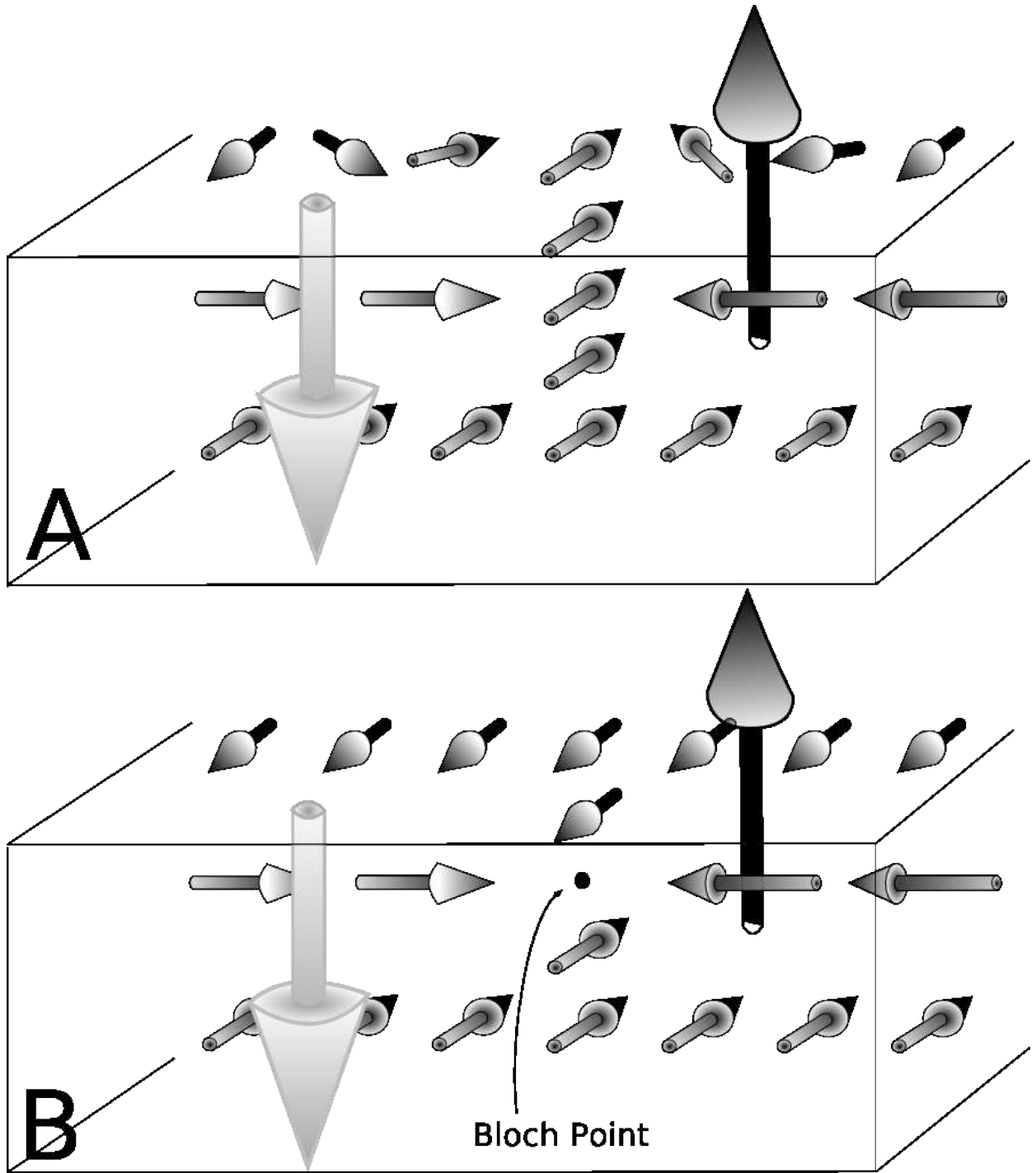


FIG. 3: (A) Vertical Bloch line without Bloch point. The upper Néel Cap of the Bloch wall is experiencing a swirl of  $360^\circ$ . (B) Vertical Bloch Lines with a Bloch point. The Néel Caps on each surface remain antiparallel.